International Journal of Engineering Applied Science and Management
ISSN (Online): 2582-6948
Vol. 3 Issue 07, July 2022

Numerical Analysis of Different Surface Material Patterns On Thermal Performance of Solar Air Heater

Daya Shankar Kumar[1] and Priyanka Jhavar[2]
M.Tech. Scholar, Department of mechanical Engineering, SSSUTMS, Sehore, M.P./466001, India[1]
Assistant Professor, Department of mechanical Engineering, SSSUTMS, Sehore, M.P./466001, India[2]

Abstract: *This work is concerned with a two-dimensional numerical study done to predict the influence of transverse rectangular cross-sectioned ribs on a solar air heater's convective heat transfer properties. Solar air heater is a useful device that can be utilized to augment the temperature of air by extracting heat from solar energy. It is a rectangular duct consisting of an absorber plate on its top and heat falls only on the top of absorber plate. When ribs/baffles are introduced just beneath the absorber plate, there is a considerable alteration in the thermal performance of air flowing through the rectangular duct. A comparison was made between the results of thin (high aspect ratio) and square ribs arranged in three patterns, namely, single wall arrangement, staggered arrangement and in-line arrangement on two opposite walls. The Nusselt number variation with Reynolds number range 5000-24000 was checked at a fixed rib pitch (p) and height (e) values. Computational fluid dynamics (CFD) simulations were performed using commercially available software ANSYS FLUENT v15.0. The results were compared with the existing experimental ones while performing simulations under similar conditions. Two methods were used to calculate the average Nusselt number in which one method extracted the local Nusselt number at many points and on averaging these, gave the average Nusselt number and the other method resembled the one used in the existing experimental work.*
The results revealed that, as compared to smooth duct, the introduction of ribs led to a considerable augmentation in heat transfer. Good agreement was found between the existing experimental results and numerical output, when the second method was adopted to calculate the Nusselt number. However, the Nusselt number calculated using method 1 yielded values lower than the existing ones. The results revealed that the thin ribs yielded better performance than the squared ones. Out of the three arrangements, the best thermal performance was given by thin inline ribs whose convective heat transfer coefficient was 1.83 times smooth duct's convective heat transfer coefficient.
Keywords: *Solar Air Heater, Absorber plate, Rectangular duct, Nusselt number, Computational fluid dynamics* .

1. Introduction

1.1 Overview of Turboexpander

Augmentation of convective heat transfer of a rectangular duct with the help of baffles/ribs has been a common practice in the past few years. This concept is widely applied in enhancing the thermo-hydrodynamic efficiency of various industrial applications such as thermal power plants, heat exchangers, air conditioning components, refrigerators, chemical processing plants, automobile radiators and solar air heaters. Solar air heater is a device used to augment the temperature of air with the help of heat extracted from solar energy. These are cheap, have simple design, require less maintenance and are eco-friendly. As a result, they have major applications in seasoning of timber, drying of agricultural products, space heating, curing of clay/concrete building components and curing of industrial products.

The shape of a solar air heater of conventional application is that of rectangular duct encapsulating an absorber plate at the top, a rear plate, insulated wall under the rear plate, a glass cover over the sun-radiation exposed surface, and a passage between the bottom plate and absorber for air to flow in. The detailed constructional details of a solar air heater are shown in fig 1.1.

Solar air heaters have higher thermal efficiency when the Reynolds number of air flow through their passage is 3000-21000. In this range, the duct flow is generally turbulent. Hence, all the research work pertaining to the design of an effective solar air heater involves turbulent flow. Conventional solar air heaters with all the internal walls being smooth usually have low efficiency. The solar air heater's internal surface can be artificially roughened by mounting certain ribs/obstacles of different shapes such as circular wires, thin rectangular bars, etc. periodically on the lower side of collector plate. This results in a considerable augmentation in the heat transfer rate, but at the same time leads to increase in friction factor thereby enhancing the pumping power requirements.

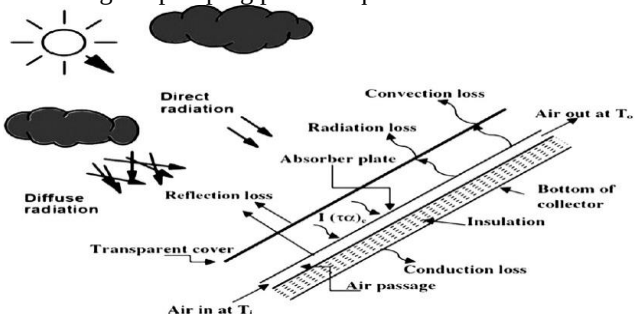

Fig. 1 Solar Air Heater Constructional Details

It is a well-known fact that the friction factor and convective heat transfer coefficient of turbulent flow are highly dependent on the surface roughness of the duct through which they pass. Hence, artificially roughened solar air heaters must be designed in such a manner that their performance yields higher convective heat transfer rates from absorber plate to air low roughness to air flow. Extensive research is being conducted in this field by many authors, whose work generally involves performing experiments or carrying out numerical simulations with different types, sizes and patterns of ribs/ baffles and finding the right parameters at which the heater gives optimal performance (minimum friction loss and maximum heat transfer). Some scientists, after performing research work on solar air heaters, develop a set of correlations for calculating Darcy's friction factor and Nusselt number in terms of operating and roughness parameters.

The mechanism by which heat transfer, between air and roughened absorber plate, increases is breakage of laminar sub-layer. The introduction of ribs leads to local wall turbulence and breakage of laminar sub-layers leading to periodic flow reattachment and separation. Vortices are formed near these baffles, which leads to a significant rise in Nusselt number.

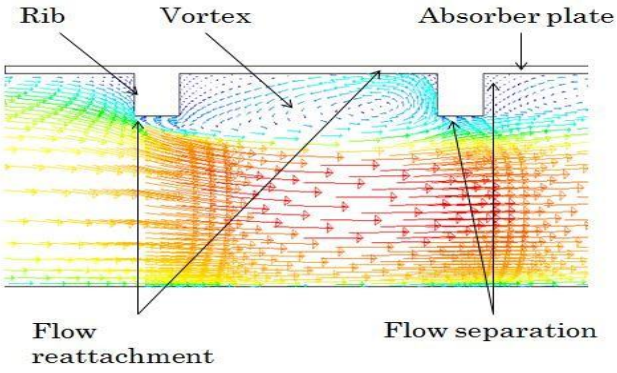

Fig. 2 Mechanism of Augmentation of Convective Heat Transfer By the Introduction of Ribs

As compared to experimental activities being carried on solar air heaters, very less numerical work has been done in this field. Numerical study of solar air heaters using CFD software is an excellent method to understand in detail how flow behaves under the presence of obstacles in solar air heaters. CFD results are more accurate as compared to experimental results. Other benefits of using CFD software's are saving of time and less costs required completing the work. Some commercially available CFD software packages are FLUENT, FLOVENT, CFX, STAR- CD and PHOENICS.

2. Related Work

Shreyas P et al. (2021) study is conducted for configurations of the absorber plate consisting of 5 mm, 8 mm, 10 mm and 12 mm vent diameters and the number of vents is varied as, 24, 36 and 54. The numerical CFD analysis is conducted for Reynolds numbers ranging from 3000 to 21,000. The CFD analysis is evaluated against the experimental results. The average increase in the thermal efficiency of 23.33% is obtained for the configuration with 8 mm diameter vents and 36 number of vents compared to the base model without the absorber plate. The average increase in thermohydraulic efficiency is 21.78% higher for the configuration with 36 vents and a vent diameter of 8 mm compared to the base model. The highest thermohydraulic efficiency of 72.8% is obtained.

The thermohydraulic efficiency of the collector is directly proportional to the increase in vent diameter. The study infers that the circular geometry and vented absorber plate causes vortex formation resulting in increase in turbulence induced heat transfer.

Mesut Abuşka et al. (2021) enhance the thermal efficiency and to create proper volume for heat storage material in terms of the effectiveness of the SAH. The thermal efficiency for the absorber with conical obstacles was 14.0, 14.6, and 11.8% higher than the flat absorber plate for the mass flow rates, respectively. The results show that the number of Nusselt obtained in conical surface experiments was highest for all cases tested regardless of Reynolds number. The experimental results are compared with the numerical results obtained by the CFD method. The model results indicate good agreement with the experimental results. Also, the results show that the heat transfer in front of the conical elements is high, and the back is low; in the smooth absorber, a linear velocity distribution is seen along the channel; however, in the conical surface absorber, the velocity distribution due to turbulence is very variable.

Vijayakumar Rajendran et al. (2021) enhance a solar air heater's performance by integrating artificial roughness through baffles on the absorber plate. In this paper, the thermal and energy matrices analysis of a Solar Air Heater (SAH) roughened with V up perforated baffles have been investigated. The effect of various mass flow rates on the SAH was analyzed with and without baffles. Experimental outputs like outlet air temperature, useful energy (heat) gain and thermal efficiency were evaluated to confirm the performance improvement. The baffled absorber plate SAH was found to give the maximum thermal efficiency and useful energy gain of 89.3% and 1321.37 W at a mass flow rate of 0.0346 kg/s, 13% and 12% higher than SAH without baffle. This result showed that the V up-shaped ribs in flow arrangement provide better thermal performance than smooth plate SAH for the parameter investigated. Energy matrices analysis and carbon dioxide mitigation of the SAH system were also analyzed.

Gandjalikhan et al. (2021) discusses the effects of flapping flexible vortex generators on two-dimensional turbulent free convection air ow in a double-pass solar air heater. To this end, two thin elastic winglets used as vortex generators were attached to two absorber walls near the inlet section at an attack angle of 65 C. This novel concept was elaborated through transient numerical simulation of the flow based on the finite element method and fluid-solid interaction. In addition, an extensive comparison of four different configurations was made in this study. The absorber and outlet temperatures as well as the ow rate and velocity field were carefully calculated, numerical results of which confirmed the considerable enhancement of thermal performance compared to that of conventional parallel double pass heater. The improvement rate was up to 54% in the case of ΔT = Tout- Tin from 13 to 20^0C while reducing the flow rate by 33.6%. The present numerical results were validated based on the experimental and numerical data reported in the literature.

Ataollah Khanlari et al. (2021) demonstrated the importance of utilizing waste materials in renewable energy-based technologies and their applicability in thermal energy production. In the first step of the analysis, the applicability of tubular-type SAHs has been studied numerically. The experiments have been conducted at two tilt angles including 90° and 32° and also at three flow rates including 0.012, 0.010, and 0.008 kg/s. The experimental findings showed that the efficiency of metal SAH and plastic SAH varied in the range of 36.33-50.96% and 31.60-47.06%, respectively. Also, enviro-economic costs for metal and plastic SAH were achieved as 8.02 and 7.55 $/year. Besides, the experimental results were predicted with ANN and SVM algorithms. The prediction success of the algorithms is discussed with four metrics (R2, MAPE, RMSE, and MBE). The outcomes clearly demonstrate the successful application of this simple and cost-effective tubular-type SAH manufactured from waste materials.

Karmveer et al. (2022) artificial roughness on the absorber of the solar air heater (SAH) is considered to be the best passive technology for performance improvement. The roughened SAHs perform better in comparison to conventional SAHs under the same operational conditions, with some penalty of higher pumping power requirements. Thermo-hydraulic performance, based on effective efficiency, is much more appropriate to design roughened SAH, as it considers both the requirement of pumping power and useful heat gain. The shape, size, and arrangement of artificial roughness are the most important factors for the performance optimization of SAHs. The parameters of artificial roughness and operating parameters, such as the Reynolds number (Re), temperature rise parameter (ΔT/I) and insolation (I) show a combined effect on the performance of SAH. In this case study, various performance parameters of SAH have been evaluated to show the effect of distinct artificial roughness, investigated previously. Therefore, thermal efficiency, thermal efficiency improvement factor (TEIF) and the effective efficiency of various roughened absorbers of SAH have been predicted. As a result, thermal and effective efficiencies strongly depend on the roughness parameter, Re and ΔT/I. Staggered, broken arc hybrid-rib roughness shows a higher value of TEIF, thermal and effective efficiencies consistently among all other distinct

roughness geometries for the ascending values of ΔT/I. This roughness shows the maximum value of effective efficiency equals 74.63% at a ΔT/I = 0.01 K·m^2/W. The unique combination of parameters p/e = 10, e/Dh = 0.043 and α = 60◦ are observed for best performance at a ΔT/I higher than 0.00789 K·m^2/W.

Asole et.al (2020) In this paper, results of CFD analysis on heat transfer and friction in rectangular ducts with broken double arc shape rib with staggered rib roughness has been presented. The rib roughness has relative roughness pitch of 10, arc angle of 30° and relative roughness height of 0.043. The relative gap position was varied from 0.30 to 0.60. The effects of relative gap position on Nusselt number, friction factor and thermo-hydraulic performance parameter have been discussed and results compared with smooth duct under similar conditions. The rough ribs were efficient enough to transfer the desired heat, but they are not economical and are very complex in design and construction. Whereas, roughness gives more area of contact.

4. Material and Methods

A rectangular section was considered. It consisted of three sections, test section of length L2, entrance section of length L1 and exit length of length L3. The domain on which numerical simulations were performed was two-dimensional. It is because they performed numerical simulations on their solar air heater of aspect ratio 7.5. They compared two dimensional results with three dimensional results on the same geometry and did not find any considerable difference between the two. They explained their observation by claiming that for continuous transverse ribs, the secondary flow effect was negligible at higher duct aspect ratios.

The geometry taken is similar to that of Skullong et al's rectangular duct. Their rectangular duct was of length 2000 mm, width 300 mm and 30 mm with a test section length of 440 mm.

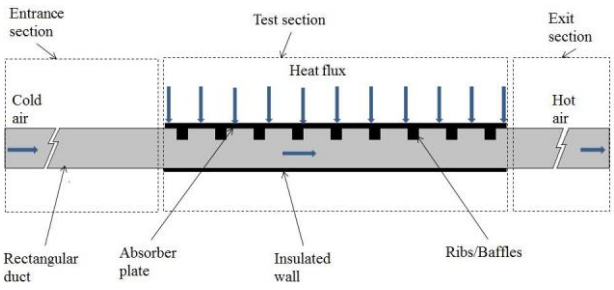

Fig. 3 Sketch of Computational Domain

Hence our domain test section length was 440 mm and its entrance and exit length dimensions were selected on the basis of ASHRAE recommendations, according to which an exit length more than $2.5\sqrt{WH}$ and entrance length more that $5\sqrt{WH}$ were compulsory to establish a fully developed flow in the test domain. The geometry of the computational domain. The different rib arrangements employed for simulation are indicated

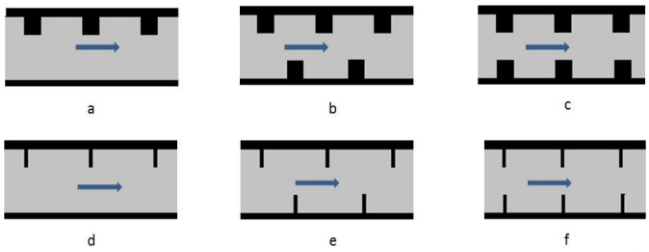

Fig. 4 Different Arrangement of Ribs Namely (A) Single Square Ribs, (B) Staggered Square Ribs, (C) In-Line Square Ribs, (D) Single Thin Ribs, (E) Staggered Thin Rib And (F) In Line Thin Ribs

Table 1: Operating and Geometrical Parameters Used For CFD Analysis

Operating and Geometrical parameters	**Value / Range**
Test length of duct, L_2	440 mm
Entrance length of duct L_1	500 mm
Exit length of duct L_3	240 mm
Duct height, H	30 mm
Duct width, W	300 mm
Duct hydraulic diameter, D_h	54.54 mm
Aspect ratio of duct, W/H	10
Constant heat flux, q"	1000 W/m^2
Range of Reynolds number	5000-23000

Repeated square ribs (tt = 6 mm) and thin ribs (tb = 0.5 mm) with an axial pitch of p = 40 mm characterized the roughness parameters of the test duct. Re was varied from 5000-23000 as this is the range in which solar air heaters particularly have higher efficiencies. Constant heat flux of value approximately 1000 W/m^2 was supplied only on the upper wall of the absorber plate. Simulations were

performed assuming the flow to be steady. The operating and geometrical parameters used for computational analysis are listed.

Governing Differential Equations

Continuity equation

$$\frac{\partial}{\partial x}(\rho u_i) = 0$$

Momentum Equation

$$\frac{\partial}{\partial x}(\rho u_i u_j) = -\frac{\partial p}{\partial x_i} + \frac{\partial p}{\partial x_i}\left[\mu\left(\frac{\partial u_i}{\partial x_j} + \frac{\partial u_j}{\partial x_i}\right) + \frac{\partial}{\partial x_j}\left(-\overline{\rho u_i' u_j'}\right)\right]$$

Energy equation

$$\frac{\partial}{\partial x}(\rho u_i T) = \frac{\partial}{\partial x_j}\left[(\Gamma + \Gamma_t)\frac{\partial T}{\partial x_j}\right]$$

Where

$\Gamma = \frac{\mu}{Pr}$ and $\Gamma = \frac{\mu_t}{Pr_t}$

Boundary Conditions

On all the walls (including the roughened one) of the rectangular duct, no-slip boundary conditions were assigned. Constant heat flux of 1000 W/m^2 was decided to be the boundary condition at the upper wall of the absorber plate. At the inlet, uniform velocity with an inlet temperature of 300 K and at the exit, invariable pressure (atmospheric pressure) boundary conditions were assigned. All the other edges were assigned as walls with insulated boundary conditions.

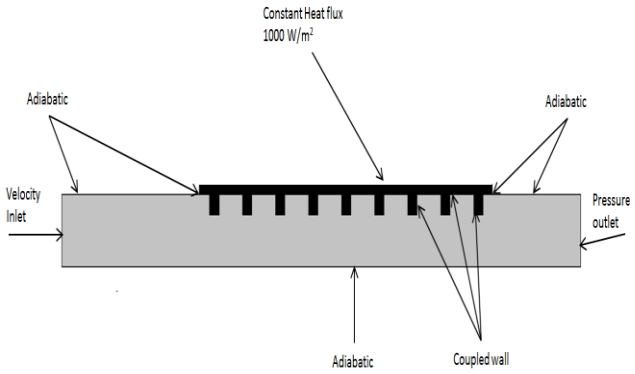

Fig. 5 Different Boundary Conditions Assigned To Edges of Computational Domain

CFD Modelling

Commercially available ANSYS FLUENT v 15.0 was the CFD software employed to solve the concerned general differential equations numerically. This software numerically simulates using

FINITE VOLUME METHOD

Construction of Geometry

The geometry was constructed in commercially available software ANSYS Design Modeler v15.0. Firstly, an outline of the geometry without ribs was created in x-y plane with appropriate dimensions (in mm) and then surface was generated from the "built sketches" option. Then another sketch that involved the interface between absorber plate and fluid was developed. The surface initially created was split into two faces with the help of "face-split" option by choosing the second sketch as the tool geometry. The face-splitting option was followed by the generation of surfaces from the faces with the help of "create surface from faces" option. Finally, all the edges and surfaces were named accordingly.

Meshing of the Domain

The meshing work was accomplished on commercially available ANSYS meshing software. The geometry created was imported in ANSYS meshing. The required number of divisions and the type of "bias" were assigned to each edge. In order to obtain regular rectangular shaped mesh cells with the best orthogonal quality, mapped facing option was activated. Finally, mesh was generated by clicking on "Generate Mesh" button. Fig. 4.4 shows the meshed domain for different cases.

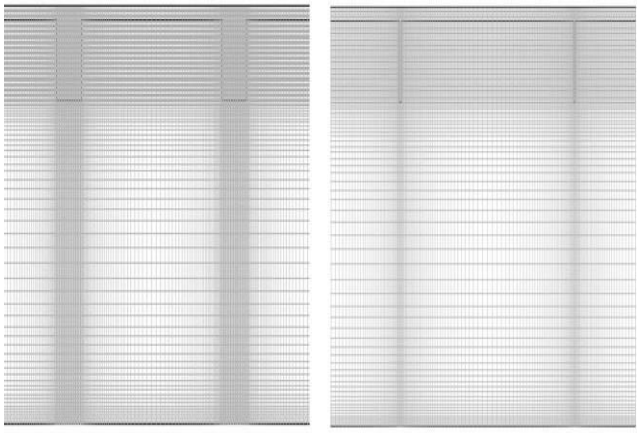

a b

Fig. 6 Details of Two-Dimensional Meshing Of (A) Single Square Ribs

The meshed domain consisted mostly of non-uniform sized cells as shown in Fig. 4.4. Fine meshing was completed near the walls in order to solve the concerned governing differential equations accurately in the laminar sub-layers at these regions. The mesh size increased towards the center. The size of the grid was constant lengthwise in entrance and exit sections of the duct and it was ensured that the maximum aspect ratio of any grid did not exceed 10.

Set Up and Flow Specification

The generated mesh was then exported to FLUENT where the different flow and physical properties were specified. The appropriate turbulent model was selected and the energy option was switched on. The working fluid was air and aluminum, because of its higher absorptive, was the absorber plate. Their thermo-physical properties are mentioned in Table 2.

Table 2 Thermo-Physical Properties of Aluminum as the Absorber Plate and Air as the Working Fluid

Properties	Working fluid (air)	Absorber plate (aluminum)
Density, kg/m^3	1.1767	2719
Viscosity, kg/m-s	1.8582e-05	-
Specific heat (constant pressure), J/kg-K	1006.6	871
Prandtl number	0.714	-
Thermal conductivity, W/m-K	0.0262	202.4

Simulations were carried out under the following assumptions

- The absorber and duct wall were assumed to be isotropic and homogenous.
- Steady, turbulent and fully developed two-dimensional-flow.
- The absorber plate and the duct wall thermal conductivity were temperature-independent.
- Negligible heat losses and no radiation heat transfer.
- At the junction of wall and fluid, no-slip boundary conditions were assumed.

The absorber plate and working fluid (air) properties were invariable at an average bulk temperature of 300 K.

4. Experimental Results

In this project, a computational model was constructed to measure a solar air heater's thermal performance. It consisted of baffles/ribs just below its absorber plate. This section presents detailed results of the average convective heat transfer characteristics.

Selection of Most Appropriate Turbulent Model

For the smooth duct, the number of mesh cells was varied from 26280 to 186880 at a Reynolds number of 22500. It was observed in simulation results using SST-k-omega and RNG-k-epsilon turbulent model, there was less than 2% alteration in average Nusselt number after 143080 number of mesh cells. When the turbulent model was Realizable-k-epsilon, there was less than 2% alteration in average Nusselt number after 105120 number of mesh cells. Hence further simulations for different Reynolds number were performed using 143080 mesh cells with SST komega and RNG-k-epsilon turbulent models and 105120 with Realizable-k-epsilon turbulence model. The Grid independence test results are represented in Fig. 5.1

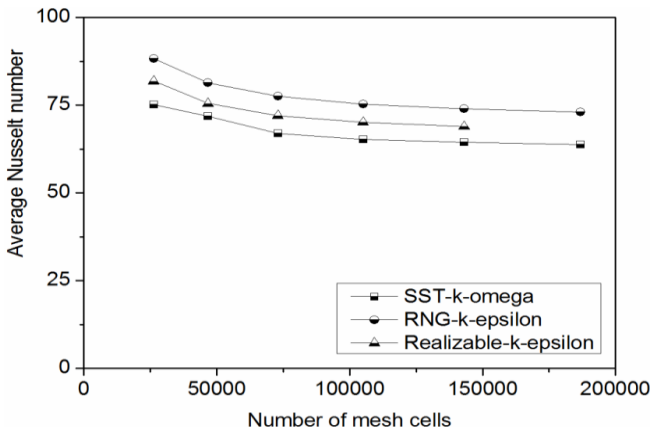

Fig. 7 Grid Independence Test Results for Selection of Most Appropriate Turbulence Model

Fig. 7 shows that as the Reynolds number incremented, the average Nusselt number increased for all the three turbulent models. The reason why this trend was observed was that as the Reynolds number increased, the flow became more turbulent (more dominance of inertial effects over viscous effects) and hence the heat transfer rate increased. Furthermore, it could be seen that the turbulent model that was the closest to output and theoretical results in the best manner was SST-k-omega. The error associated was less than 3 %. Hence, SST-komega turbulent model was used for simulating the roughened ducts.

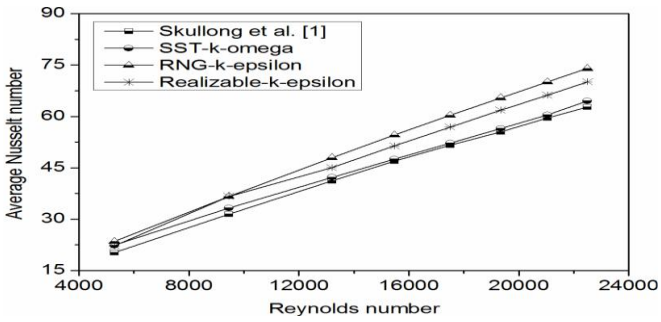

Fig. 8 Comparison of Smooth Duct Results for Different Turbulent Models

Numerical Simulations On Ducts with Different Shaped Ribs

This section presents detailed results of average convective heat transfer characteristics of the heater, for different shaped ribs.

Grid Independence test results for all the different geometries

Figure 9 shows the results of grid independence tests conducted on different geometries. The turbulent model used was SST-k-omega for all the cases, since in the previous section it was proved that SST-k-omega most accurately simulated a solar air heater. The best mesh size was extracted from the Grid Independence test when there was less than 2 % variation in results on further increasing the number of mesh cells after this mesh size. Table 4.1 gives the range in which the number of mesh cells was varied and the most appropriate number of mesh cells for each configuration.

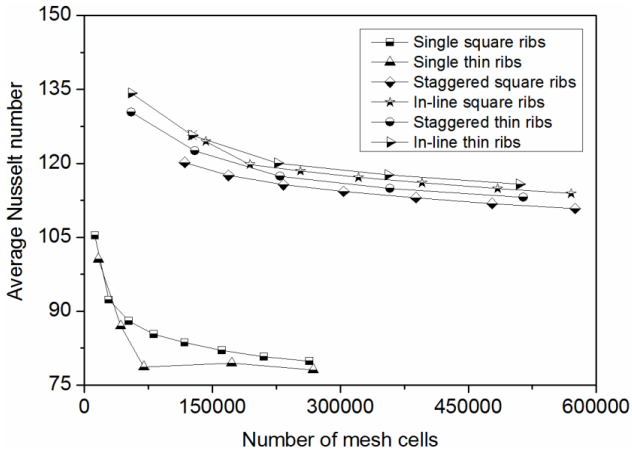

Fig. 9 Grid Independence Test Results For Different Rib Arrangements

Table 3 Grid Independence Test Results

Rib configuration	Range of mesh cells	Best number of mesh cells
Single square	12516 – 268396	210636
Single thin	16500 – 268366	172620
Staggered square	117644 – 575320	477864
In-line square	142316 - 570576	484284
Staggered thin	55048 – 514568	357962
In-line thin	54934 - 509856	355882

Simulation for different roughened ducts at different Reynolds number

The best grid sizes were obtained by performing grid independence tests whose results wereexplained in the previous section. The average convective Nusselt number was measured usingtwo methods. The first method (method-1) is given by equation and takes the average of all.

The local Nusselt numbers along the test section length. The second method (method-2) used and it is the most widely employed method of calculating Nusselt number in experimental works. The second method was used clearly depicts the outcome of average Nusselt number alteration with Re for the geometries separately. As Re was raised, the average Nusselt number increased for all cases. The reason why this trend was observed was that as the Re was raised, the flow became more turbulent (more dominance of inertial effects over viscous effects) and hence the heat transfer rate increased.

There was a decent agreement when numerical outputs were compared with the experimental ones existing in the literature. Excellent matching between Nusselt numbers calculated using method 2 and the existing ones was observed for square ribs but good agreement was found incase of thin ribs.

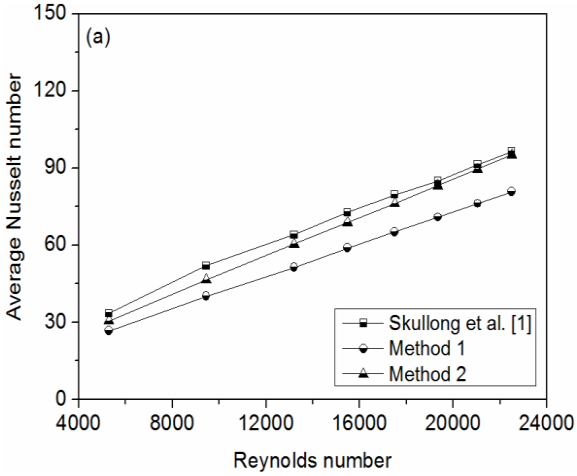

(A) Single Square Ribs

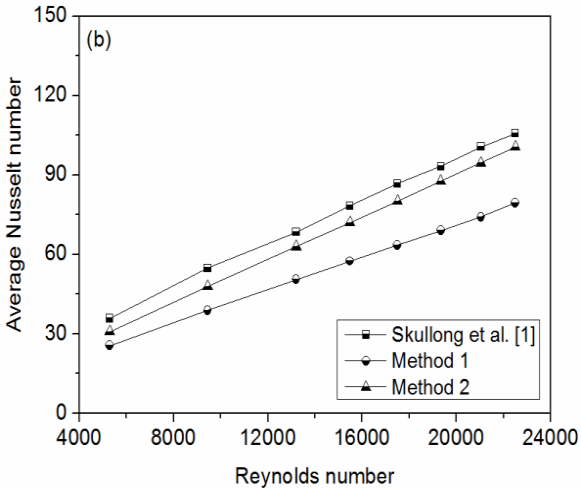

(B) Single Thin Ribs

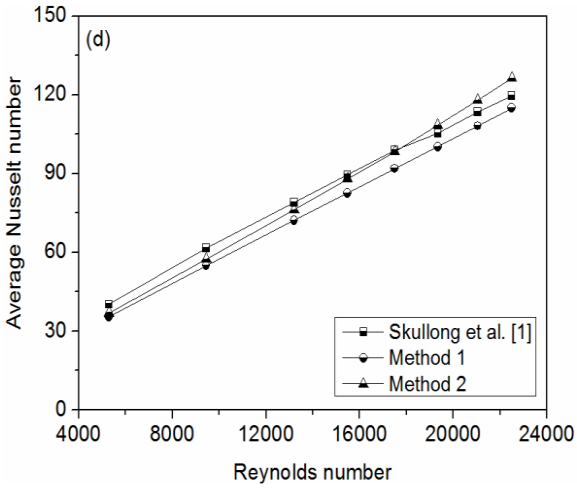

(C) Staggered Square Ribs

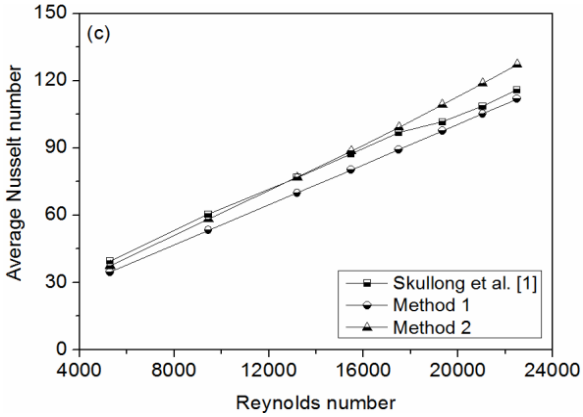

(D) In-Line Square Ribs

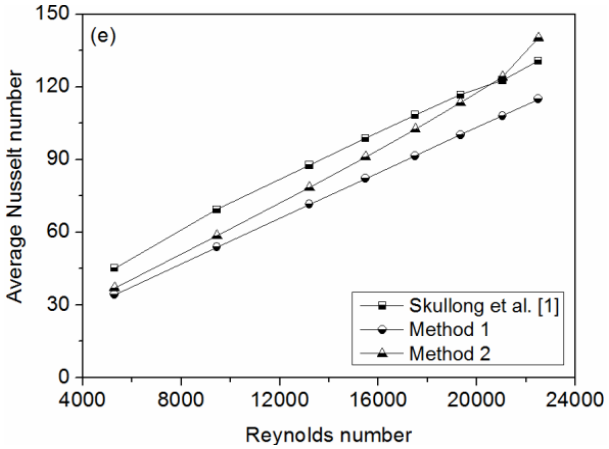

(E) Staggered Thin Ribs

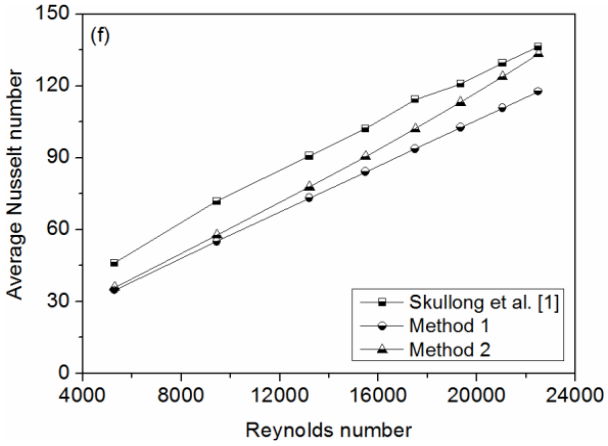

(F) Inline Thin Ribs.

Fig. 10 Results Of Numerical Analysis At Different Reynolds Number

The percentage deviation of numerical results using method-2 from experimental results was found to be approximately 5, 8.3, 5, 7.4, 8.5 and 11.4 for solar air heaters with single square ribs, single thin ribs, staggered square ribs, in-line square ribs, staggered thin ribs and in-line thin ribs respectively.
Nusselt number calculated using method-1 was observed to be considerably lower than the experimental ones for all the case. The corresponding percentage deviations were calculated as18.7, 27, 3.3, 7.4, 17 and 18.3 for solar air heaters with single square ribs, single thin ribs, staggered square ribs, in-line square ribs, staggered thin ribs and in-line thin ribs respectively.

Comparison of Nusselt number variation with Reynolds number for all the geometries

Fig 11 graphically outlines a comparison between Nusselt number and Reynolds number for all the geometries. It can be inferred from the graph that there was a considerable augmentation in Nusselt number for both thin as well as square ribs. Interestingly, thin ribs gave much better thermal performance than their square counterparts. In-line gave the highest Nusselt number for the complete Reynolds number range used in this simulation. The possible reason attributed to this phenomenon is due to the strong interruption of flow and diversion of its direction by in-line thin baffles. The ribbed configurations in the increasing order of Nusselt number are single thin ribs, single square ribs, staggered square ribs, in-line square ribs, thin staggered ribs and thin inline ribs. The same pattern was observed in the experimental results of except that single thin ribs in the present work gave the lowest Nusselt numbers.

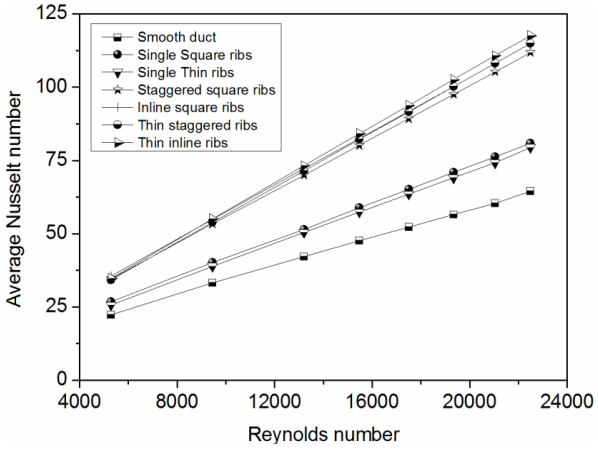

Fig. 11 Variation of Nu with Re for All the Cases

Nusselt number enhancement (Nu/Nu_0) versus Reynolds number for separate geometries

Nusselt number enhancement ratio gives information about the increment in Nusselt number of a solar air heater with ribs from that of a smooth one. Fig. 5.6 gives a comparison Nusselt number enhancement alteration with Re for all the arrangements. In-line thin ribs yielded the best Nusselt number enhancement ratio.
The maximum Nu/Nu0 values with square ribs were 1.26, 1.74, 1.79 for single, staggered and in-line patterns respectively and those with thin ribs were 1.23, 1.79 and1.83 respectively thereby clearly indicating that thin ribs have advantage over the square ones. The highest value of Nu/Nu_0 was observed for thin-in line ribs at Re = 21040. In the experimental work of Skullong et al. the maximum Nu/Nu0 values with square ribs were1.52, 1.81 and 1.86 1.74 for single, staggered and in-line patterns respectively and those with thin ribs were 1.64, 2.05 and 2.13 respectively.

Table 4

Nu/Nu0 when Re=21040			
Nusselt		**Skullong**	
Square Ribs	**Thin Ribs**	**square ribs**	**Staggered and thin ribs**
1.26	1.23	1.52	1.64
1.74	1.79	1.81	2.05
1.79	1.83	1.86	2.13

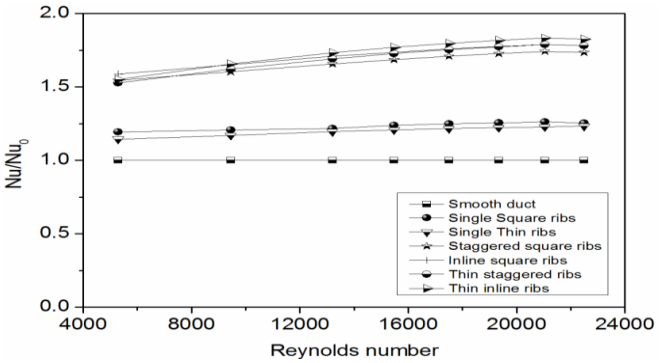

Fig. 12 Variation of Nu/Nu0 with Re For All The Cases

5. Conclusion and Future Work

A two-dimensional numerical analysis is done to predict the influence of transverse rectangular cross-sectioned ribs on a solar air heater's convective heat transfer properties.

A rectangular duct was constructed and numerical analysis was carried out on square and thin (high aspect ratio) rib shapes arranged in different fashion, namely single wall, staggered and in-line ribs arranged on two opposite walls including the absorber plate. Air was the working fluid and constant heat flux was applied only on the absorber plate's top surface. The output of numerical simulations drew the following conclusions

- On comparing simulation results, pertaining to smooth duct's average Nusselt number, for different turbulent models, it was found that SST-k-omega can best predict the thermal performance of the solar air heater.
- For all the cases considered in this work, increase in Reynolds number leads to augmentation in Nusselt number.
- When ribs/baffles are introduced just beneath the collector plate, there was a considerable alteration in the heat transfer coefficient of air.
- Two methods is used to calculate the average Nusselt number in which one method extracted the local Nusselt number at many points and on averaging these, gave the average Nusselt number and the other method resembled the one used in the existing experimental work. Good matching between existing experimental results and numerical outputs was spotted, when the second method was adopted to calculate the Nusselt number, thereby proving that CFD can be effectively applied for the design of solar air heaters. However the Nusselt number calculated using first method yielded values lower than the existing ones.
- The staggered ribs gave lower Nusselt number than the in-line ones.
- Out of the three arrangements, the best thermal performance was given by thin inline ribs whose convective heat transfer coefficient was 1.83 times that of smooth duct.

Since, it is observed that high aspect ratio ribs allow higher convective heat transfer, hence it would be interesting to conduct research work on triangular shaped ribs having very low apex angles. The present work is expected to be very helpful for carrying out the new future project.

References

[1] Faris Aissaoui et al. , "Numerical study on thermal performance of a solar air collector with fins and baffles attached over the absorber plate", International Journal Of Heat And Technology, Vol. 35, No. 2, June 2017, pp. 289-296 DOI: 10.18280/ijht.350209.

[2] Shreyas P et al. "Numerical analysis of a solar air heater with circular perforated absorber plate", Solar Energy Volume 215, February 2021, Pages 416-433.

[3] Mesut Abuşka and Arif Kayapunar, "Experimental and numerical investigation of thermal performance in solar air heater with conical surface", Heat and Mass Transfer 2021, 57(11):1-16 DOI:10.1007/s00231-021-03054-5.

[4] [Vijayakumar Rajendran et al., "Performance analysis of domestic solar air heating system using V-shaped baffles – An experimental study", Sage Journal 2021, Volume: 235 issue: 5, page(s): 1705-1717.

[5] Devi Prasad Asole, Sandeep Kumar Shah, numerical investigation of solar air heater duct using broken double arc shaped ribs combined with staggered rib piece, IJARIIE- ISSN(O)-2395-4396, vol-6 issue-1 2020.

[6] Gandjalikhan et al. (2021), "Novel design of natural double-pass solar air heater for higher thermal performance using vortex generator", Sharif University of Technology Scientia Iranica Transactions B: Mechanical Engineering http://scientiairanica.sharif.edu

[7] Rahul Kumar and Sujit Kumar Verma, "Exergetic And Energetic Evaluation Of An Innovative Solar Air Heating System Coated With Graphene And Copper Oxide Nanoparticles", Journal of Thermal Engineering, Vol. 7, No. 3, pp. 447-467, March, 2021 Yildiz Technical University Press, Istanbul, Turkey.

[8] Ataollah Khanlari et al. , "Numerical And Experimental Analysis Of Longitudinal Tubular Solar Air Heaters Made From Plastic And Metal Waste Materials", Heat Transfer Research, 2021, Volume 52, Issue 10, 2021, pp. 19-45 DOI: 10.1615/HeatTransRes.2021038204.

[9] Karmveer et al., "The Effect of Roughness in Absorbing Materials on Solar Air Heater Performance", Materials 2022, 15, 3088. https:// doi.org/10.3390/ma15093088.

[10] Gawande, V.B.; Dhoble, A.S.; Zodpe, D.B.; Chamoli, S. Experimental and CFD investigation of convection heat transfer in solar air heater with reverse L-shaped ribs. Sol. Energy 2016, 131, 275–295. [CrossRef]

[11] Kumar, A.; Layek, A. Nusselt number and friction characteristics of a solar air heater that has a winglet type vortex generator in the absorber surface. Int. Commun. Heat Mass Transf. 2012, 39, 634–639. [CrossRef]

[12] Kumar, A.; Layek, A. Nusselt number and friction factor correlation of solar air heater having winglet type vortex generator over absorber plate. Sol. Energy 2020, 205, 334–348. [CrossRef]

[13] Patel, Y.M.; Jain, S.V.; Lakhera, V.J. Thermo-hydraulic performance analysis of a solar air heater roughened with reverse NACA profile ribs. Appl. Therm. Eng. 2020, 170, 114940. [CrossRef]

[14] Kumar, A.; Layek, A. Energetic and exergetic performance evaluation of solar air heater with twisted rib roughness on absorber plate. J. Clean. Prod. 2019, 232, 617–628. [CrossRef]
[15] Promvonge, P.; Khanoknaiyakarn, C.; Sripattanapipat, S.; Skullong, S. Heat transfer in solar air duct with multi-V-ribbed absorber and grooved back-plate. Chem. Eng. Res. Des. 2021, 168, 84–95. [CrossRef]